International Journal of Current Advanced Research
ISSN: O: 2319-6475, ISSN: P: 2319 – 6505, Impact Factor: SJIF: 5.995
Available Online at www.journalijcar.org
Volume 6; Issue 9; September 2017; Page No. 5743-5747
DOI: http://dx.doi.org/10.24327/ijcar.2017.5747.0791

Research Article

ADAPTIVE THRESHOLDING WAVELET BASED DENOISING USING WHALE OPTIMIZATION ALGORITHM

***[1]Neha Bharti, [2]Richa Upadhyay, [3]Kirti Choudhary and [4]Geetika Gautam**

[1]Department of Information Technology, RCEW, Jaipur, India.
[2,4] Department of Computer Science & Engineering, JECRC, Jaipur , India
[3]Department of Computer Science &Engineering, Jagannath University, Jaipur, India

ARTICLE INFO

Article History:

Received 19th June, 2017
Received in revised form 3rd July, 2017 Accepted 18th August, 2017
Published online 28th September, 2017

Key words:

Image denoising; discrete wavelet transform; hard and soft thresholding; WOA; Gaussian noise; peak signal to noise ratio.

ABSTRACT

Generally images have poor contrast along with serious types of noises. The suppression of noise in medical images corrupted by Gaussian white noise is a major issue in diverse image processing and computer vision problems. Image denoising systems are important for accurate clinical diagnosis. The purpose of this study is to present a simple and effective iterative multistep image denoising system based on adaptive wavelet transform (AWT) using whale optimization algorithm where the denoised image from one stage is the input to the next stage. The denoising process stops when a particular condition measured by image energy is adaptively achieved. The proposed scheme is tested on images and performance is measured by the well-known peak-signal-to-noise-ratio (PSNR) and SSIM statistic. Proposed algorithm has been validated through ultrasound image corrupted by a variety of noise densities through Gaussian noise. Simulation results show that the proposed method outperforms the existing denoising methods.

INTRODUCTION

Image enhancement and denoising are usually used to better visualize and interpret the content [1–6]. In this regard, several effective denoising systems for enhancement of biomedical images corrupted with noise during acquisition process have been proposed in the literature. The main goal of biomedical image denoising is to suppress noise from acquired image while preserving as much as possible its meaningful edges or texture details. Indeed, the accuracy of clinical diagnosis depends mainly on visual quality of acquired images. For instance, wavelet-based approach was adopted in [7], partial differential equation was employed in [8,9], adjusted empirical mode decomposition in [10], nonlocal means in [11], and Wiener filter was used in [12]. As a suitable filter to reduce the effects of non-stationary noise, Wiener filter was successful in denoising one and two dimensional biomedical signals [13,14], and also in image processing in general [15]. Recently, several iterative approaches were proposed in the literature to denoise images. For instance, an iterative method based on fuzzy sub-pixel fractional partial difference was proposed in [16]. The proposed iterative method was successful in enhancing contrast of noisy image. However, it is a computationally complex method [16]. An iterative generalized cross-validation and fast translation invariant approach for image denoising was proposed in [17].

Corresponding author:* **Neha Bharti
Department of Information Technology, RCEW, Jaipur, India,

The approach is based on wavelet thresholding algorithm and found to be fast and effective as it reduces the computation cost of the standard generalized cross-validation method and efficiently suppresses the Pseudo-Gibbs phenomena. However, it yields to slight blurring due to simplicity of the soft-threshold function which is necessary to accelerate computation. The authors in [18] proposed a noise adjusted iterative low-rank matrix approximation method. For instance, a patchwise randomized singular value decomposition is first applied to denoise the image. Then, an iterative regularization technique based on low-rank matrix approximation is employed to further separate the signal and noise. The proposed algorithm requires an appropriate stopping parameter to be pre-determined along with number of iterations. More recently, the authors in [19] proposed an automatic filtering convergence method using PSNR checking and filtered pixel detection for iterative impulsenoise filters by defining an adaptive stop criterion to filter a corrupted image within finite steps. However, the improved iterative impulse noise filters fail to discriminate both impulse noise and high-frequency signal contained in high-frequency image.

In this paper, a simple and effective multistep system for image denoising based on Wiener filtering is presented. The Wiener filter is chosen as the basis of our proposed multistep denoising system for three reasons. First, it is effective in reducing the effects of nonstationary noise [14]. Second, it incorporates both the degradation function and statistical characteristics of noise into the restoration process [15]. Third, it can remove the additive noise and invert the blurring

simultaneously [15]. The proposed multistep system for image denoising based on Wiener filtering is described as follows. In the first step, the Wienerfilter is applied to the noisy image. In the second step, the obtained denoised image in previous step is processed by Wiener filter for improving image quality by removing the remaining noise. The resulting denoised image in second step is further processed by Wiener filter in third step. In other words, the proposed denoising system is composed of several stages/steps where each obtained denoised image is further processed with Wiener filter. The process continues until obtaining a better quality of the image. For instance, the multistep processing stops when a given condition is automatically satisfied.

In order to evaluate the proposed multistep denoising system, a set of three biomedical images is considered. In particular, the real clinical test images are degraded by various levels of Gaussian noise. In addition, the effectiveness of the proposed multistage denoising system is compared with that of conventional existing methods; including wavelet packet (WP) [20], fourth order partial differential equation (PDE) [21], nonlocal Euclidean mean (NLEM) [22], and first order local statistics (FOLS) [23]. Finally, the performances of all algorithms will be evaluated in terms of the well-known peak-signal-to-noise ratio (PSNR).The remainder of this paper is organized as follows: Section 2 presents our proposed multistep denoising system along with comparison techniques. Section 3 presents the experimental results. Finally, Section 4 concludes our study.

Wavelet Transform Denoising

When the useful signal is transformed by wavelet, the energy will concentrate on the small number of wavelet coefficients. At the same time, noise will be distributed on the entire time axis at all-time scales due to the not related wavelet coefficients. In the processing, other points value will be set as zero or reduced maximum, and the processed wavelet would be inverse transformed. Then, noise will be suppressed. Threshold denoising is based on the comparison of transform domain coefficients and threshold value, and processed coefficient should be transformed to reconstruct the denoising image. Concrete steps of wavelet threshold denoising method are shown as the following:

- ***Step 1:*** wavelet decomposition of the image: Determine the wavelet function and decomposition levels, and decompose the image with layer wavelet.
- ***Step 2:*** Threshold selection: select the threshold for each wavelet coefficients of each layer, and judge the threshold of detail coefficients.
- ***Step 3:*** Image reconstruction: coefficient with threshold processed will be used to reconstruct the image by inverse wavelet transform.

The signal and noise have different correlation in wavelet domain. The wavelet coefficients of the signal have a strong correlation at the corresponding positions, while the coefficients of the noise are weakly related or not related. Scale correlation denoisingis using different correlation characteristics of the image signal and noise in wavelet transform domain. Comparing the two denoising algorithms, they adopt different approaches to wavelet coefficients. Threshold denoising uses the “horizontal” process method. It firstly selects the threshold, and then compared to the wavelet coefficients. In the threshold denoising method, due to the fixed threshold, it will not change with the wavelet coefficients, which leads the inevitably error on the part of the wavelet coefficients. When the threshold is properly selected, most error coefficients will appear in the neighborhood of threshold. In the adjacent region of the threshold, there will be less error wavelet coefficients according to scale correlation estimation. So, scale correlation estimation method used for the wavelet coefficients can reduce the error and improve the accuracy of the wavelet coefficient threshold judgment. There is no doubt that it will be more effectively for image denoising.

Modified Threshold Denoising Algorithm

The improved threshold based improved wavelet denoising of infrared image can be divided into some steps:
Step 1: Wavelet decomposition: decomposition of the image with layers wavelet discretion;
Step 2: Threshold processing: modified threshold processing scheme will be used to determine the threshold size, and new threshold function would be used to deal with the wavelet coefficients;

Step 3: Image reconstruction: reconstruct the image by inverse wavelet transformation.

Objective function
Root Mean Square Error

It will be nearly zero when the reference and fused images are alike and it will increase when the dissimilarity increases.

$$RMSE = \sqrt{\frac{1}{MN}\sum_{x=1}^{M}\sum_{y=1}^{N}\left(I_r(x,y) - I_f(x,y)\right)^2}$$

2. PSNR qualities
It gives upgraded esteem when the fused and true or genuine images are indistinguishable and superior value entails superior fusion.
It's equation is given by

$$\boldsymbol{PSNR = 20\log_{10}\left(\frac{L^2}{\sqrt{\frac{1}{MN}\sum_{x=1}^{M}\sum_{y=1}^{N}\left(I_r(x,y) - I_f(x,y)\right)^2}}\right)}$$

Here, L indicates the number of gray levels.

SSIM values [8]
It is a Measure of Structural Similarity Index. Regular image signals would be very organized and their pixels reveal strong dependencies. These dependencies would convey essential data about the structure of the object. Local patterns of pixel intensities are compared that have been standardized for luminance and difference.

$$\boldsymbol{SSIM = \frac{\left(2\mu_{I_r}\mu_{I_f} + C_1\right)\left(2\sigma_{I_rI_f} + C_2\right)}{\left(\mu_{I_r}^2 + \mu_{I_r}^2 + C_1\right)\left(\sigma_{I_r}^2 + \sigma_{I_r}^2 + C_2\right)}}$$

Where C_1 is a constant that is included to avoid the instability when $\mu_{I_r}^2 + \mu_{I_r}^2$ is close to zero and C_2 is a constant that is included to avoid the instability when $\sigma_{I_r}^2 + \sigma_{I_r}^2$ is close to zero.

Whale Optimization Algorithm (WOA)

According to Hof and Van Der Gucht, whales have com-mon cells in certain areas of their brains similar to those of human called spindle cells. These cells are responsible for judgment, emotions, and social behaviors in humans.

Mathematical model and optimization algorithm

In this section the mathematical model of encircling prey, spiral bubble-net feeding maneuver, and search for prey is first provided. The WOA algorithm is then proposed.

Encircling prey

Humpback whales can recognize the location of prey and encircle them. Since the position of the optimal design in the search space is not known a priori, the WOA algorithm assumes that the current best candidate solution is the target prey or is close to the optimum. After the best search agent is defined, the other search agents will hence try to update their positions towards the best search agent. This behavior is represented by the following equations:

$$\vec{D} = \left| \vec{C} . \vec{X}*(t) - \vec{X}(t) \right| \quad (3.1)$$

$$\vec{X}(t+1) = \vec{X}*(t) - \vec{A}.\vec{D} \quad (3.2)$$

where t indicates the current iteration, A and C are coefficient vectors, X^* is the position vector of the best solution obtained so far, X is the position vector, $|\ |$ is the absolute value, and $\cdot$ is an element-by-element multiplication. It is worth mentioning here that X^* should be updated in each iteration if there is a better solution.

The vectors A and C are calculated as follows:

$$\vec{A} = 2\vec{a}.\vec{r} - \vec{a} \quad (3.3)$$

$$\vec{C} = 2.\vec{r} \quad (3.4)$$

where $\vec{a}$ is linearly decreased from 2 to 0 over the course of iterations (in both exploration and exploitation phases) and $\vec{r}$ is a random vector in [0,1]. The position (X, Y) of a search agent can be updated according to the position of the current best record (X^*,Y^*). Different places around the best agent can be achieved with respect to the current position by adjusting the value of $\vec{A}$ and $\vec{C}$ vectors.

It should be noted that by defining the random vector $\left(\vec{r}\right)$ it is possible to reach any position in the search space located between the key-points.

Therefore, Eq. (3.2) allows any search agent to update its position in the neighborhood of the current best solution and simulates encircling the prey. The same concept can be extended to a search space with n dimensions, and the search agents will move in hyper-cubes around the best solution obtained so far. As mentioned in the previous section, the humpback whales also attack the prey with the bubble-net strategy. This method is mathematically formulated as follows:

Bubble-net attacking method (exploitation phase)

In order to mathematically model the bubble-net behavior of humpback whales, two approaches are designed as follows:

Shrinking encircling mechanism: This behavior is achieved by decreasing the value of $\vec{a}$ in the Eq. (3.3). Note that the fluctuation range of $\vec{A}$ is also decreased by $\vec{a}$. In other words is a random value in the interval [$-a$, a] where a is decreased from 2 to 0 over the course of iterations. Setting random values for $\vec{A}$ in [−1,1], the new position of a search agent can be defined anywhere in between the original position of the agent and the position of the current best agent. The possible positions from (X, Y) towards ($X*$, $Y*$) that can be achieved by $0 \leq A \leq 1$ in a 2D space.

Spiral updating position

This approach first calculates the distance between the whale located at (X, Y) and prey located at ($X*$, $Y*$). A spiral equation is then created between the position of whale and prey to mimic the helix-shaped movement of humpback whales as follows:

$$\vec{X}(t+1) = \vec{D'}.e^{bl}.\cos(2\pi l) + \vec{X}*(t) \quad (3.5)$$

Where $\vec{D'} = \left| \vec{X}*(t) - \vec{X}(t) \right|$ indicates the distance of the i^{th} whale to the prey (best solution obtained so far), b is a constant for defining the shape of the logarithmic spiral, l is a random number in [−1,1], and . is an element-by-element multiplication.

Note that humpback whales swim around the prey within a shrinking circle and along a spiral-shaped path simultaneously. To model this simultaneous behavior, we assume that there is a probability of 50% to choose between either the shrinking encircling mechanism or the spiral model to update the position of whalesduring optimization. The mathematical model is as follows:

If (p<0.5)

$$\vec{X}(t+1) = \vec{X}*(t) - \vec{A}.\vec{D} \quad (3.6.1)$$

If(p≥ 0.5)

$$\vec{X}(t+1) = \vec{D'}.e^{bl}.\cos(2\pi l) + \vec{X}*(t) \quad (3.7.2)$$

where$p$ is a random number in [0,1].

Search for prey (exploration phase)

The same approach based on the variation of the A vector can be utilized to search for prey (exploration). In fact, humpback whales search randomly according to the position of each other. Therefore, we use A with the random values greater than 1 or less than −1 to force search agent to move far away from a reference whale. In contrast to the exploitation phase, we update the posi- tion of a search agent in the exploration phase according to a ran- domly chosen search agent instead of the best search agent found so far. This mechanism and | A | > 1 emphasize exploration and al- low the WOA algorithm to perform a global search. The mathemat- ical model is as follows:

$$\vec{D} = \left| \vec{C} \cdot \vec{X}_{rand} - \vec{X} \right| \quad (3.7)$$

$$\vec{X}(t+1) = \vec{X}_{rand} - \vec{A} \cdot \vec{D} \quad (3.8)$$

Algorithm 1: Whale Optimization Algorithm
Set the initial value of the whales population Xi (i = 1, 2,..... n), Parameter a, Coefficient Vector A, C, and he maximum number of iteration Max_{itr}
Set t=0 {Counter Initialization}
for (i=1: 1≤ n)
    Generate an initial population $X_i(t)$ randomly.
    Calculate the fitness of each search agent $f(X_i)$
Assign the best search agent $X_i(t)$
while (t < maximum number of iterations)
for (i=1: 1≤ n)
Update a, A, C, l, and p
if1 (p<0.5)
  if2 (|A| < 1)
    Update the position of the current search agent by the Eq. (3.1)
  else if2 (|A| ≥ 1)
    Select a random search agent (X_ rand)
    Update the position of the current search agent by the Eq. (3.8)
  end if2
else if1 (p ≥0.5)
    Update the position of the current search by the Eq. (3.5)
end if1
end for
Check if any search agent goes beyond the search space and amend it
Calculate the fitness of each search agent, X*=the best search agent
Update X* if there is a better solution
t=t+1
end while
return X*

Figure 1: Whale Optimization Algorithm

Where $\overrightarrow{X_{rand}}$ is a random position vector (a random whale) chosen from the current population.

The WOA algorithm starts with a set of random solutions. At each iteration, search agents update their positions with respect to either a randomly chosen search agent or the best solution obtained so far. The 'a' parameter is decreased from 2 to 0 in order to provide exploration and exploitation, respectively. A random search agent is chosen when $|\overrightarrow{A}| > 1$, while the best solution is selected when $|\overrightarrow{A}| < 1$ for updating the position of the search agents. De- pending on the value of p, WOA is able to switch between either a spiral or circular movement. Finally, the WOA algorithm is terminated by the satisfaction of a termination criterion.

The pseudo code of the WOA algorithm is presented in Fig. 1. From theoretical stand point, WOA can be considered a global optimizer because it includes exploration/exploitation ability. Furthermore, the proposed hyper-cube mechanism defines a search space in the neighborhood of the best solution and allows other search agents to exploit the current best record inside that domain. Adaptive variation of the search vector *A* allows the WOA algorithm to smoothly transit between exploration and exploitation: by decreasing *A*, some iterations are devoted to exploration ($|A| \geq 1$) and the rest is dedicated to exploitation ($|A| < 1$). Remarkably, WOA includes only two main internal parameters to be adjusted (*A* and *C*).

RESULTS AND DISCUSSION

Consider Image 'cameraman.png' for image denoising as original image and added salt and pepper noise in original image and obtained noisy cameraman image. Set the parameter for whale optimization algorithm and apply this algorithm with adaptive wavelet transform on this image. Unknown parameters are level of decomposition, wavelet choice, and thresholding values for optimization. The lower and upper limits of unknown parameters are considered and run the algorithm to obtain values for maximum output of objective function. The objective function is consisting of PSNR and SSIM quality matrices.

Table 1 Quality Analysis of Proposed Image denoising Scheme

S.No.	Quality Matrices	Original Image	Denoised Image
1	PSNR	34.3359	34.3431
2	SSIM	0.6025	0.6056

Figure 2 (a) Original Image (b) Noisy image

The search agents 0 and maximum iteration are 20 and 150 respectively for WOA algorithm.

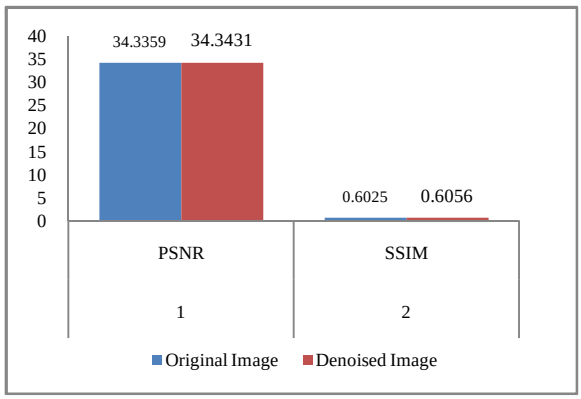

Figure 3 Comparative Study between Original and Denoised Image

CONCLUSION

This paper deals with adaptive wavelet transform based image denoising scheme. For adaptivity of wavelet transform, whale optimization algorithm is used to obtained level of decomposition, wavelet choice, and thresholding values for wavelet transform. The effectiveness of proposed scheme is shown by table and plots.

References

1. M.K. Sharma, J. Joseph, P. Senthilkumaran, Directional edge enhancement using superposed vortex filter, *Opt. Laser Technol.* 57 (2014) 230-235.
2. X. Bai, F. Zhou, B. Xue, Image enhancement using multiscale image features extracted by top-hat transform, *Opt. Laser Technol.* 44 (2012) 328-336.
3. Y. Li, Y. Zhang, A. Geng, L. Cao, J. Chen, Infrared image enhancement based on atmospheric scattering model and histogram equalization, *Opt. Laser Technol.* 83 (2016) 99-107.

4. H. Om, M. Biswas, MMSE based map estimation for image denoising, *Opt. Laser Technol*. 57 (2014) 252-264.
5. P. Shanmugavadivu, K. Balasubramanian, Particle swarm optimized multi-objective histogram equalization for image enhancement, *Opt. Laser Technol*. 57 (2014) 243-251.
6. M. Liao, Y.-q.Zhao, X.-h.Wang, P.-s. Dai, Retinal vessel enhancement based on multi-scale top-hat transformation and histogram fitting stretching, *Opt. Laser Technol.* 58 (2014) 56-62.
7. T. Bernas, R. Starosolski, R. Wójcicki, Application of detector precision characteristics for the denoising of biological micrographs in the wavelet domain, Biomed. Signal Process. *Control* 19 (2015) 1-15.
8. J.M. Bioucas-Dias, M.A.T. Figuiredo, Multiplicative noise removal using variable splitting and constrained optimization, IEEE Trans. Image Process. 19 (2010) 1720–1730.
9. S. Lahmiri, Image denoising in bidimensional empirical mode decomposition domain: the role of Student's probability distribution function, Healthc. Technol. Lett. 3 (2016) 67-71.
10. S.Lahmiri, M.Boukadoum, Combined partial differential equation filtering and particle swarm optimization for noisy biomedical image segmentation, in: Proceedings of the IEEE Latin American Symposium on Circuits and Systems, pp. 363-366, 2016.
11. S. Duli, A. Kuurstra, I.C.S. Patarroyo, O.V. Michailovich, A new similarity measure for non-local means filtering of MRI images, *J. Vis. Commun. Image Represent.* 24(2013) 1040-1054.
12. X.-W. Fu, M.-Y. Ding, C. Cai, Despeckling of medical ultrasound images based on quantum-inspired adaptive threshold, Electron. Lett. 46 (2010) 889-891.
13. L. Smital, M. Vítek, J. Kozumplík, I. Provazník, Adaptive wavelet Wiener filtering of ECG signals, *Trans. Biomed. Eng*. 60 (2013) 437-445.
14. Q. Xu, D. Ye, Evaluation of a posteriori Wiener filtering applied to frequency following response extraction in the auditory brainstem. Biomedical, Signal Process. *Control* 14 (2014) 206-216.
15. J.-C. Yoo, C.W. Ahn, Image restoration by blind-Wiener filter, IET Image Process. 8(2014) 815-823.
16. Y. Zhang, H.D. Cheng, J. Tian, J. Huang, X. Tang, Fractional subpixel diffusion and fuzzy logic approach for ultrasound speckle reduction, *Pattern Recognit.* 43 (2010) 2962-2970.
17. Libao Zhang, Jie Chen, Tong Zhu, Image denoising based on iterative generalized cross-validation and fast translation invariant, *J. Vis. Commun*. Image Represent. 28 (2015) 1-14.
18. W. He, H. Zhang, L. Zhang, H. Shen, Hyperspectral image denoising via noiseadjusted iterative low-rank matrix approximation, IEEE *J. Sel. Top. Appl. Earth Obs. Remote Sens*. 8 (2015) 3050-3061.
19. C.-Y. Chen, C.-H.Chen, C.-H.Chen, K.-P. Lin, An automatic filtering convergence method for iterative impulse noise filters based on PSNR checking and filtered pixels detection, *Expert Syst. Appl.* 63 (2016) 198-207.
20. P.L. Shui, Z.F. Zhou, J.X. Li, Image denoising algorithm via best wavelet packet base using Wiener cost function, IET Image Process. 1 (2007) 311-318.
21. Y.-L. You, M. Kaveh, Fourth order partial differential equations for noise removal, IEEE Trans. Image Process. 9 (2000) 1723-1730.
22. D. Sheet, S. Pal, A. Chakraborty, J. Chatterjee, A.K. Ray, Image quality assessment for performance evaluation of despeckle filters in optical coherence tomography of human skin, Proc. IEEE EMBS (2010) 499-504.
23. J.S. Lee, Digital image smoothing and sigma filter, Comput. Vis. Graph. *Image Process.* 24 (1983) 255-269.

How to cite this article:

Neha Bharti *et al* (2017) 'Homocysteine Thiolactone Forms Covalent Adduct With Arginine And Histidine ', *International Journal of Current Advanced Research*, 06(09), pp. 5743-5747. DOI: http://dx.doi.org/10.24327/ijcar.2017.5747.0791

****